Artificial Channels in an Infectious Biofilm Created by Magnetic Nanoparticles Enhanced Bacterial Killing by Antibiotics

Quan, Kecheng; Zhang, Zexin; Chen, Hong; Ren, Xiaoxiang; Ren, Yijin; Peterson, Brandon W.; van der Mei, Henny C.; Busscher, Henk J.

Published in:
Small

DOI:
10.1002/smll.201902313

NANO · MICRO small
www.small-journal.com

Artificial Channels in an Infectious Biofilm Created by Magnetic Nanoparticles Enhanced Bacterial Killing by Antibiotics

Kecheng Quan, Zexin Zhang, Hong Chen, Xiaoxiang Ren, Yijin Ren, Brandon W. Peterson, Henny C. van der Mei,* and Henk J. Busscher**

The poor penetrability of many biofilms contributes to the recalcitrance of infectious biofilms to antimicrobial treatment. Here, a new application for the use of magnetic nanoparticles in nanomedicine to create artificial channels in infectious biofilms to enhance antimicrobial penetration and bacterial killing is proposed. *Staphylococcus aureus* biofilms are exposed to magnetic-iron-oxide nanoparticles (MIONPs), while magnetically forcing MIONP movement through the biofilm. Confocal laser scanning microscopy demonstrates artificial channel digging perpendicular to the substratum surface. Artificial channel digging significantly (4–6-fold) enhances biofilm penetration and bacterial killing efficacy by gentamicin in two *S. aureus* strains with and without the ability to produce extracellular polymeric substances. Herewith, this work provides a simple, new, and easy way to enhance the eradication of infectious biofilms using MIONPs combined with clinically applied antibiotic therapies.

Bacterial infections are predicted to become the number one cause of death in the year 2050.[1] Bacterial infections are mainly due to bacteria in a biofilm mode of growth,[1] in which inhabitants are protected against antimicrobial treatment.[2,3] This protection largely arises due to limited penetration of antimicrobials through the biofilm, killing only those bacteria residing at the biofilm surface.[4] This appears to be a stubborn problem, persisting ever since its first description by Van Leeuwenhoek in the 17th century.[5] Moreover, the intrinsic resistance to antibiotics many bacterial strains and species have acquired after the discovery of penicillin by Flemming[6] adds to our inability to control infectious bacterial biofilms.[7,8] Biofilms are surface-adhering and surface-adapted communities of bacteria,[9] embedded in a self-produced matrix of extracellular polymeric substances (EPS). In order to allow effective diffusion of autoinducers, nutrients, and waste products, water-filled channels and pores exist in biofilms.[10] Water-filled channels and pores naturally develop in biofilms by a variety of mechanisms.[3] Motile bacillus swimmers, for example, have the ability to dig water-filled channels by flagella-propelled movement. By irrigating pathogenic *Staphylococcus aureus* biofilms with bacillus swimmers, artificial channels in staphylococcal biofilms have been created that make these infectious biofilms 100 times more susceptible to benzalkonium chloride.[11] Although an elegant pathway to enhance efficacy of current antimicrobials, clinical translation is difficult as it would involve adding another potentially pathogenic strain in an already infected patient. Yet, the idea is highly interesting from an engineering point of view. In nanomedicine, magnetic nanoparticles are used in magnetic resonance imaging, magnetically targeted drug delivery, and control of magnetic hyperthermia because of their excellent biocompatibility.[12] Antimicrobial magnetic nanoparticles are frequently suggested as a new strategy to combat infectious biofilms.[13–15] However, actual magnetic targeting into a biofilm, antimicrobial loading and release, or creating antimicrobial magnetic particles is not trivial.[16] Inspired by the ability of bacillus swimmers to create channels in biofilms, we here forward the use of magnetic nanoparticles as a new, nonbiotic method to create artificial channels in an infectious biofilm in order to improve penetration and enhance bacterial killing by antimicrobials (see **Figure 1**).

To test our hypothesis that magnetic nanoparticles can be used to dig artificial channels in biofilms to enhance antimicrobial penetration and bacterial killing by antimicrobials, we first prepared magnetic iron oxide nanoparticles (MIONPs).[17] The size distribution of MIONPs was measured by dynamic light scattering (DLS; **Figure 2**a) and both transmission (TEM;

K. Quan, Prof. Z. Zhang, Prof. H. Chen
College of Chemistry
Chemical Engineering and Materials Science
Soochow University
Suzhou 215123, P. R. China
E-mail: zhangzx@suda.edu.cn
K. Quan, X. Ren, Dr. B. W. Peterson, Prof. H. C. van der Mei, Prof. H. J. Busscher
Department of Biomedical Engineering
University of Groningen and University Medical Center Groningen
9713 AV Groningen, The Netherlands
E-mail: h.c.van.der.mei@umcg.nl; h.j.busscher@umcg.nl
Prof. Y. Ren
Department of Orthodontics
University of Groningen and University Medical Center Groningen
9713 GZ, Groningen, The Netherlands
The ORCID identification number(s) for the author(s) of this article can be found under https://doi.org/10.1002/smll.201902313.

DOI: 10.1002/smll.201902313

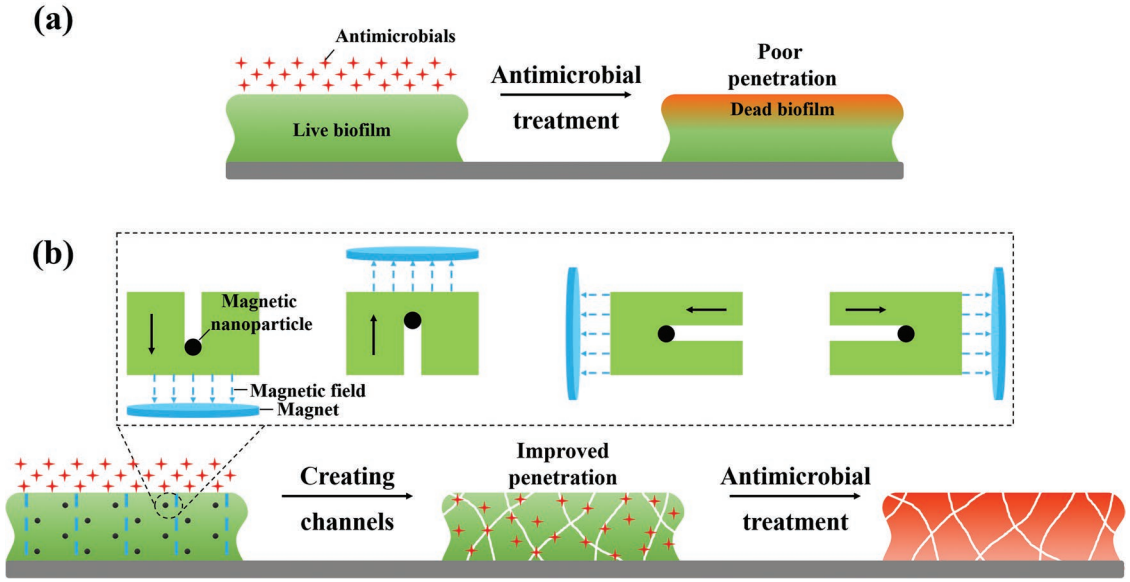

Figure 1. Schematics of our hypothesis that magnetic nanoparticles can be used to engineer artificial channels in infectious biofilms to improve antimicrobial penetration and enhance bacterial killing over the depth of a biofilm. Details not drawn to scale. a) Biofilms are poorly penetrable by antimicrobials and often only bacteria at the biofilm surface are killed by antimicrobial treatment, while bacteria residing in deeper layers of a biofilm survive antimicrobial treatment, adding to the recalcitrance of bacterial infections against antibiotic treatment. b) Inspired by the natural ability of highly motile bacteria to dig channels for the transport of autoinducers, nutrients, and waste products through a biofilm, we hypothesize that by moving magnetic nanoparticles through a biofilm perpendicular and parallel to a substratum surface, artificial channels can be created that improve antimicrobial penetration and enhance bacterial killing over the depth of a biofilm.

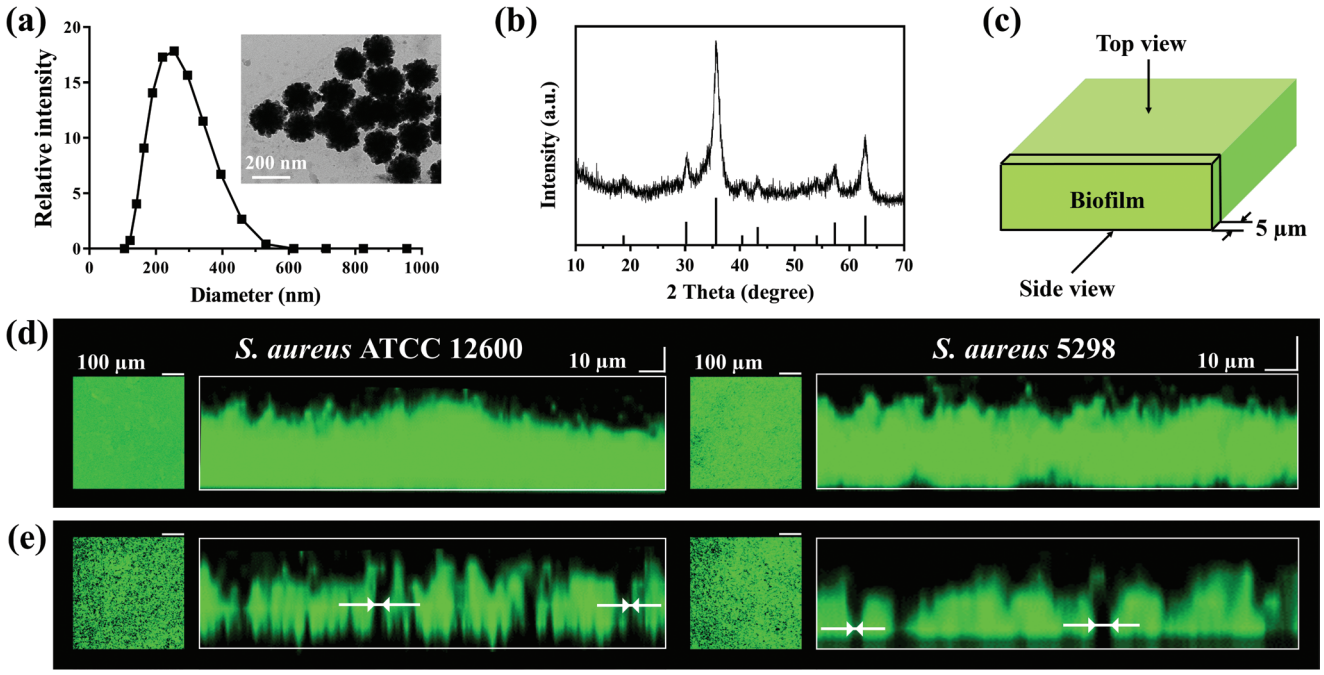

Figure 2. a) Example of the diameter distribution of MIONPs in PBS (pH 7.4), determined by dynamic light scattering, together with a transmission electron microscopy image of the MIONPs employed in this study. b) X-ray diffraction pattern of the MIONPs used. c) Schematics of the procedure applied to obtain overlayer and transverse cross-sectional images of a biofilm in confocal laser scanning microscopy (CLSM). d) Overlayer and transverse cross-sectional CLSM images of 24 h old *S. aureus* ATCC 12600 and *S. aureus* 5298 biofilms prior to artificial channel digging by MIONPs (500 µg mL^{-1}). e) Same as panel (d), but after digging artificial channels by moving MIONPs according to the pattern shown in Figure 1b. Magnetic channel digging (9 min) was initiated after adding 1000 µL of a MIONP suspension (500 µg mL^{-1}) to the well, in which a biofilm was grown. Channels perpendicular to the substratum surface appear as black dots on the green-fluorescent biofilms. Channel widths were measured in cross-sectional images, as indicated by white arrows.

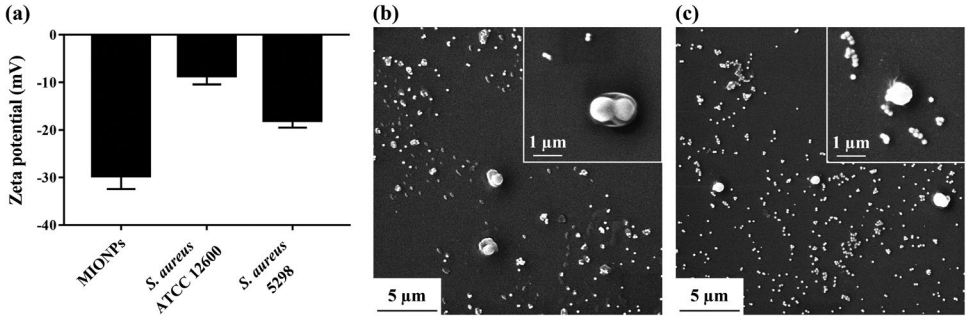

Figure 3. a) Zeta potentials of the MIONPs and *S. aureus* strains used, as measured in PBS (pH 7.4). Zeta potentials are expressed as means ± standard deviations over three separate experiments with different nanoparticles and differently cultured bacteria. b) Scanning electron microscopy images, demonstrating absence of interactions between MIONPs and EPS producing *S. aureus* ATCC 12600 after 9 min exposure to a MIONP suspension (500 µg mL^{-1}). c) Same as (b), now for non-EPS producing *S. aureus* 5298.

Figure 2a) and scanning electron microscopy (SEM; Figure S1a, Supporting Information). DLS yielded an average hydrodynamic diameter over triplicate experiments of 278 ± 61 nm (± is full width at half maximum of the distribution), corresponding to TEM and SEM images. DLS furthermore showed that the hydrodynamic diameter of MIONPs increased upon exposure to 10% serum or tryptone soy broth (Figure S1b, Supporting Information), but this was not statistically significant within the variation observed within one suspension ($p > 0.05$, Student's two-tailed *t*-test). The structure of the MIONPs analyzed by X-ray diffraction (XRD; Figure 2b) corresponded with literature data on similarly prepared iron oxide nanoparticles,[17] while their magnetic properties were confirmed by vibrating sample magnetometry (VSM; Figure S1c, Supporting Information) and also found similar to literature.[17] (2,3-Bis-(2-methoxy-4-nitro-5-sulfophenyl)-2H-tetrazolium-5-carboxanilide salt) (XTT) conversion of human fibroblasts grown in absence and presence of MIONPs (Figure S2, Supporting Information) demonstrated no harmful effects on cellular viability.

Next, *S. aureus* biofilms were grown in 12-well plates. *S. aureus* is one of the most common pathogens in a variety of severe human infections.[18] Since the EPS matrix can provide a biofilm with viscoelastic properties that might affect artificial channel creation, two strains of *S. aureus* were employed: a strain with (ATCC 12600) and without (5298) the ability to produce EPS.[19,20] After 24 h of growth, staphylococcal biofilms were stained with SYTO 9 and confocal laser scanning microscopy (CLSM) images were taken (Figure 2c). Averaged over three separately grown biofilms of each strain, the thickness of *S. aureus* ATCC 12600 and *S. aureus* 5298 amounted 44 ± 9 and 34 ± 8 µm, respectively (not significantly different: $p > 0.05$, Student's two-tailed *t*-test). These thicknesses coincide with the thickness of clinically occurring biofilms.[21] Untreated staphylococcal biofilms prior to magnetically forcing MIONP movement through, appeared highly compact (Figure 2d), both in overlayer as well as in transverse cross-sectional images, with no demonstrable channels or pores. After magnetically forcing MIONPs to move through a biofilm according to the pattern outlined in Figure 1b, the thickness of the biofilms decreased to 38 ± 11 and 26 ± 3 µm for *S. aureus* ATCC 12600 and *S. aureus* 5298, respectively, but these do not represent significant decreases ($p > 0.05$, Student's two-tailed *t*-test). Artificial channels were created perpendicular to the substratum surface (visible as the black regions in top views and optical cross sections, compare Figure 2d and 2e), but unexpectedly no visible channels could be created parallel to the surface. Likely magnetic forces could not push or pull magnetic nanoparticles against the biofilm mass in a direction parallel to the surface, as this represents a much larger mass displacement than particles moving perpendicular to the surface have to dig through. Moreover, this suggests absence of direct interaction between MIONPs and staphylococci in the biofilms due to electrostatic double-layer repulsion between negatively charged MIONPs and staphylococci (**Figure 3**a). SEM confirms that electrostatic double-layer repulsion inhibited direct interaction between staphylococci and MIONPs (Figure 3b,c). Channel widths were measured from transverse cross-sectional CLSM images (see Figure 2d,e) and found to be 1.4 ± 1.0 µm for *S. aureus* ATCC 12600 and 1.3 ± 0.7 µm for *S. aureus* 5298 (means ± standard deviations over ten different images) which is larger than the diameter of individual nanoparticles, due to aggregation of the nanoparticles in suspension (see also Figure 2a).

In a separate series of experiments, staphylococcal biofilms were exposed to phosphate buffered saline (PBS) at a MIONP concentration of 500 µg mL^{-1} without or with magnetically forced movement in absence or presence of gentamicin. Gentamicin is a clinically applied antibiotic in local delivery devices, which can yield extremely high local concentrations up to 4000 µg mL^{-1}, such as in the narrow interfacial gap of total hip arthroplasties between bone and bone cement.[22] Its clinical application as a locally applied antibiotic makes it a potential candidate for use in combination with artificially dug channels to combat infectious biofilms, which is the reason why it has been chosen for proof of principle in this study. After exposure to PBS as a control or MIONPs, biofilms were removed from the well surfaces and suspended in PBS. The resulting bacterial suspension was partly plated on agar for colony forming units (CFU) enumeration, while enumeration of the total number of staphylococci (dead and alive) was done using a Bürker-Türk counting chamber.

Relative to PBS without MIONPs, MIONPs without or with magnetically forced movement in absence of gentamicin (0 µg mL^{-1}) did not significantly ($p > 0.05$, Student's two-tailed *t*-test) decrease the number of CFUs in the staphylococcal biofilms (**Figure 4**a,b) nor the total number of staphylococci (Figure 4c,d), regardless of the staphylococcal strain involved. This confirms absence of direct interaction between MIONPs and the staphylococci.

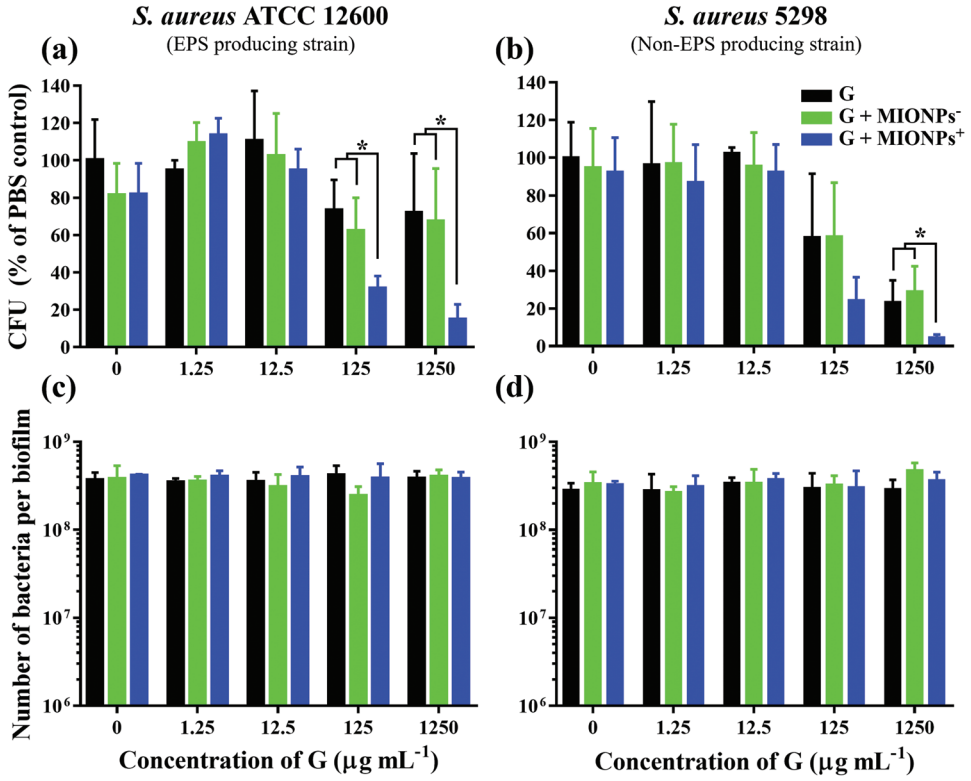

Figure 4. a) Numbers of CFUs after exposure to MIONPs (500 μg mL^{-1}) without or with 9 min magnetically forced movement in absence (0 μg mL^{-1} gentamicin) or presence of different concentrations of gentamicin for *S. aureus* ATCC 12600. CFUs are expressed in percentages relative to the number of CFUs after 3 h exposure of staphylococcal biofilms to PBS (0 μg mL^{-1} gentamicin) in a 12-well plate. b) Similar as (a), now for *S. aureus* 5298. c,d) Similar to (a) and (b), respectively, now for total counts. G denotes gentamicin, $MIONPs^{-}$ and $MIONPs^{+}$ denote absence and presence of magnetically forced nanoparticle movement, respectively. Data are expressed as means ± standard deviations over three separate experiments. Statistical analysis was performed using the Student's two-tailed *t*-test (*$p < 0.05$).

Exposure of the staphylococcal biofilms to gentamicin only also yielded no significant ($p > 0.05$, Student's two-tailed *t*-test) decrease in CFUs nor total counts for *S. aureus* ATCC 12600 over the entire range of gentamicin concentrations evaluated (up to 1250 μg mL^{-1}), due to the protection offered by its EPS produced. However, *S. aureus* 5298 was more susceptible to gentamicin in its biofilm mode of growth due to its inability to produce a protective EPS matrix and a significant ($p < 0.05$, Student's two-tailed *t*-test) decrease in CFUs set-in at a gentamicin concentration of 1250 μg mL^{-1}. Since total counts were not decreased, this indicates that staphylococci killed by the antibiotic, remained part of the biofilm.

Additionally, the presence of MIONPs in absence of magnetically forced movement had no significant ($p > 0.05$, Student's two-tailed *t*-test) effect on this reduction, but for gentamicin concentration ≥ 125 μg mL^{-1} magnetically forced MIONP movement caused a 4–6-fold stronger reduction in CFUs by gentamicin in both strains, but again, not in total counts. Thus, forcing magnetic movement of MIONPs is essential in achieving the higher antibiotic penetration and bacterial killing observed. The concentration at which MIONPs are forced to move plays only a marginal role (Figure S3, Supporting Information).

This demonstrates that our hypothesis forwarded in Figure 1 is correct and therewith an entirely new way to employ magnetic nanoparticles for the control of infectious biofilms arises. Importantly, the improved penetration of existing antibiotics through nonbiotically created artificial channels allows to use these antibiotics more effectively for the control of biofilms in combination with forced magnetic MIONP movement that might otherwise appear antibiotic-resistant in absence of artificially dug channels due to lack of penetration.

The absence of antimicrobial modification of the magnetic nanoparticles applied in artificial channel digging presents an advantage with respect to clinical translation, both in terms of regulatory approval and economic feasibility.[23] Phage conjugation to magnetic nanoparticles, for instance, has been demonstrated to effectively reduce biofilm formation by *Pseudomonas aeruginosa* and *Escherichia coli* in vitro,[13] but its clinical application would raise many concerns due to the inclusion of phages.[24,25] Dual-catalytic magnetic iron oxide nanoparticles have recently been demonstrated to break down biofilm exopolysaccharide matrices and allow subsequent removal of fragmented biofilm debris via magnetically forced nanoparticle movement.[14] This highly elegant method however still leaves biofilm inhabitants alive after fragmentation of the biofilm and debris removal, while moreover it requires sophisticated, highly precise control of magnetic movement. Channel digging as proposed here combined with exposure to existing antibiotics not only kills biofilm inhabitants, but also does not require precise magnetic targeting but only relatively rough control of forced

nanoparticle movement through a biofilm. Precise targeting of magnetic nanoparticles in a biofilm is not easy and often magnetic nanoparticles are hypothetically pictured in schematics to distribute homogeneously over the depth of a biofilm[15] and to remain there for antimicrobial action. It can be doubted whether such precise control of antimicrobial-nanoparticle distribution over the depth of an infectious biofilm can be easily achieved under clinical conditions. The absence of the need to precisely move and position nanoparticles in a biofilm is a clear advantage of artificial channel digging by non-antimicrobial MIONPs in combination with antibiotic treatment as proposed here.

In conclusion, artificial channels have been successfully created in *S. aureus* biofilms by magnetically forcing nanoparticles to move through the biofilm. Staphylococcal killing by gentamicin was significantly (4–6-fold) enhanced through improved penetration of gentamicin through the artificial channels. Since MIONPs have been demonstrated here and described in the literature as fully biocompatible,[26] the current observations should be further advanced to clinical application. Moreover, there are no reasons to assume why the advantages of magnetically dug, artificial channels in biofilms would be confined to gentamicin. Last but not least, the use of magnetic nanoparticles is highly preferable above the use of bacterial swimmers to create artificial channels[11] that might cause infection themselves.

Experimental Section

Materials: Gentamicin and iron (III) chloride ($FeCl_3{\cdot}6H_2O$) were purchased from Aldrich. Trisodium citrate dehydrate ($C_6H_5O_7Na_3{\cdot}2H_2O$), urea, polyacrylamide (PAM, 300 kDa), and glutaraldehyde (50%, v/v) were purchased from Sinopharm Chemical Reagent Co. All chemicals were used as received.

Preparation and Characterizations of MIONPs: MIONPs were synthesized as previously described[17] by dissolving $FeCl_3{\cdot}6H_2O$ (0.54 g, 2 mmol), $C_6H_5O_7Na_3{\cdot}2H_2O$ (1.18 g, 4 mmol), and urea (0.36 g, 6 mmol) in 40 mL distilled water and stirring for 10 min. Then PAM (0.3 g, 7.5 g L^{-1}) was added under stirring for 30 min. The solution was transferred into a 100 mL Teflon-lined stainless-steel autoclave. The autoclave was sealed and maintained at a temperature of 200 °C for 12 h. After cooling down to room temperature, the black precipitate was magnetically separated and washed with water and ethanol separately, each for three times. Finally, the black powder obtained was dried in vacuum overnight. For further use, MIONPs were suspended in distilled water under sonication (Transonic TP 690, ELMA, Germany, 160 W, 35 kHz) at room temperature for 30 min. The size and shape of MIONPs were determined using TEM (G-120, Hitachi, Japan) and SEM (S-4700, Hitachi, Japan). Wide-angle powder XRD patterns were recorded using an X'Pert-Pro MPD diffractometer (PANalytical, The Netherlands) with a Cu Kα X-ray source (λ = 1.540598 Å). The magnetic property of MIONPs was investigated at room temperature by VSM (model 7410, Lake Shore, USA) measurements. The hydrodynamic diameters of MIONPs were measured by DLS (Malvern ZetaSizer ZS2000, UK) and the charge of MIONPs was measured by zeta potentials (Malvern ZetaSizer ZS2000, UK). SEM was used to observe the interactions between MIONPs and *S. aureus*.

Biocompatibility Evaluation: Biocompatibility of MIONPs was evaluated using an XTT conversion assay.[27] Briefly, human fibroblasts (American Type Culture Collection ATCC-CRL-2014) were cultured in a 96-well plate at a seeding density of 5×10^3 cells per well in 100 µL cell growth medium (Dulbecco's modified Eagle's medium (DMEM, ThermoFisher Scientific)) supplemented with 10% fetal bovine serum (FBS; Invitrogen). After 24 h incubation under 5% CO_2 at 37 °C, 100 µL MIONPs suspended in medium were added at different concentrations (250, 500, and 1000 µg mL^{-1}). After subsequent growth for 24 h, 50 µL XTT (AppliChem) reagent solution combined with activation solution (PMS (n-methyl dibenzopyrazine methyl sulfate), Sigma-Aldrich)) was added. XTT and activation solutions were prewarmed to 37 °C and incubation pursued for another 4 h at 37 °C. Next, absorbance $A_{485\ nm}$ was measured using a photo-spectrophotometer (Shimadzu, Japan). According to the manufacturer's instructions, $A_{690\ nm}$ was measured and subtracted as a reference control. The viability of the fibroblasts after MIONP exposure was calculated relative to one of the cells exposed to PBS (5×10^{-3} M K_2HPO_4, 5×10^{-3} M KH_2PO_4, 150×10^{-3} M NaCl, pH 7.4) in absence of MIONPs according to

$$\text{Relative viability}(\%) = \frac{A_{\text{MIONPs 485 nm}} - A_{\text{MIONPs 690 nm}}}{A_{\text{PBS 485 nm}} - A_{\text{PBS 690 nm}}} \times 100\% \quad (1)$$

Biofilm Growth: *S. aureus* ATCC 12600 and *S. aureus* 5298 were grown from a frozen stock solution (7 v/v% DMSO) overnight on a blood agar plate at 37 °C. Then, one colony was transferred from the agar plate into 10 mL tryptone soy broth (TSB; OXOID, Basingstoke, U.K.) and incubated for 24 h at 37 °C. This preculture was subsequently transferred into 200 mL TSB. After 16 h of incubation at 37 °C, staphylococcal cultures were harvested by centrifugation (5000 × g, 5 min, 10 °C) followed by washing twice in sterilized PBS. Next, cultures were sonicated 3 times for 10 s (Vibra cell model 375, Sonics and Material Inc., Danbury, CT) under immersion in an ice/water bath to obtain a suspension with single bacteria. The concentration of the suspension was adjusted to 1×10^9 bacteria mL^{-1}, as determined in a Bürker-Türk counting chamber. The suspension was put in sterile 12-well polystyrene plates for 2 h at room temperature in order to allow bacterial adhesion. Thereafter, the wells were washed 3 times with sterile PBS, filled with fresh TSB, and incubated for 24 h at 37 °C.

Creation of Artificial Channels through Magnetically Forced Movement of MIONPs: After 24 h growth of the staphylococci in 12-well plates, the growth medium was removed and the biofilm was washed by 1 mL PBS. Next, 1000 µL MIONPs suspension (500 µg mL^{-1}) was added to each well and a disc NdFeB magnet (10 mm diameter, 1 mm height, 1.17-1.21 Tesla residual magnetism) was first pressed to the bottom of the well for 1 min and subsequently placed 1 min above each well to force magnetic movement of the nanoparticles perpendicular to the substratum surface. Next, the magnet was circled around the well to force nanoparticle movement through the biofilm parallel to the substratum surfaces, also for 1 min (see also Figure 1b). Magnetically forced movement of nanoparticles was repeated three times according to the above cycle.

Staphylococcal biofilms with artificial channels dug by MIONPs were stained with SYTO 9 (Thermo Fisher Scientific, Waltham, MA) for 15 min in the dark and subsequently imaged using CLSM (Leica TCS SP2 Leica, Wetzlar, Germany) with a HCX APO L40×/0.80 W U-V-I objective. An argon ion laser at 488 nm was used to excite the SYTO 9 and fluorescence was collected at 500–540 nm. CLSM images were acquired and analyzed using Leica software, version 2.0. The top view of the biofilm was made by stacking images layer by layer using ImageJ software. The transverse, cross-sectional view of the biofilm had thickness of 5 µm (see also Figure 2b).

In a separate experiment, staphylococcal biofilms were grown in order to study the effect of gentamicin on biofilms with artificially created channels. After 24 h of growth, the medium was removed and the biofilm was washed by 1 mL PBS. Next, biofilms were exposed to 0.5 mL of gentamicin at different concentrations up to 1250 µg mL^{-1}, well above the minimal bactericidal concentration of planktonic staphylococci (MBC, 1.1 ± 0.7 µg mL^{-1}), and MIONPs (500 µg mL^{-1}) were added to the biofilms and channels were created, as described above. An equivalent volume of PBS with and without MIONPs in absence of magnetically forced movement was taken as a control. Subsequently, growth was pursued for another 3 h at 37 °C after which the exposed biofilms were gently washed with 500 µL PBS to remove MIONPs and gentamicin. Finally, staphylococcal biofilms were dispersed and suspended in PBS for enumeration of CFUs and total (live and dead) counts (see next for details).

CFU and Total Count Enumeration: For CFU enumeration, biofilms were dispersed by forcefully pipetting PBS repeatedly in the wells and

collecting the fluid that was subsequently vortexed in order to obtain single, dispersed staphylococci. Suspensions of dispersed staphylococci were serially diluted in PBS and each dilution was inoculated on a TSB agar plate and incubated for 16 h at 37 °C for CFU enumeration or injected in a Bürker-Türk counting chamber for immediate enumeration of total counts.

Statistics: All comparisons of CFUs and total counts of staphylococci in differently treated biofilms were performed using a two-tailed Student's *t*-test, accepting significance value of 0.05.

Supporting Information

Supporting Information is available from the Wiley Online Library or from the author.

Acknowledgements

This work was financially supported by National Key Research and Development Program of China (2016YFC1100402), the National Natural Science Foundation of China (21334004, 11574222 and 21522404), and UMCG, Groningen, The Netherlands.

Conflict of Interest

H.J.B. is also director of a consulting company, SASA BV (GN Schutterlaan 4, 9797 PC Thesinge, The Netherlands). The authors declare no potential conflicts of interest with respect to authorship and/or publication of this article. Opinions and assertions contained herein are those of the authors and are not construed as necessarily representing views of their respective employers.

Keywords

antibiotic penetration, biofilm channels, biofilm eradication, gentamicin, iron-oxide nanoparticles

Received: May 7, 2019
Revised: July 11, 2019
Published online:

[1] G. Humphreys, F. Fleck, *Bull. W. H. O.* **2016**, *94*, 938.
[2] H. C. Flemming, J. Wingender, U. Szewzyk, P. Steinberg, S. A. Rice, S. Kjelleberg, *Nat. Rev. Microbiol.* **2016**, *14*, 563.
[3] H. C. Flemming, J. Wingender, *Nat. Rev. Microbiol.* **2010**, *8*, 623.
[4] D. Davies, *Nat. Rev. Drug Discovery* **2003**, *2*, 114.
[5] A. van Leeuwenhoek, *Philos. Trans. R. Soc. London* **1684**, *14*, 568.
[6] A. Flemming, *Br. J. Exp. Pathol.* **1929**, *10*, 226.
[7] T. Bjarnsholt, O. Ciofu, S. Molin, M. Givskov, N. Høiby, *Nat. Rev. Drug Discovery* **2013**, *12*, 791.
[8] H. Koo, R. N. Allan, R. P. Howlin, P. Stoodley, L. H. Stoodley, *Nat. Rev. Microbiol.* **2017**, *15*, 740.
[9] C. B. Whitchurch, T. T. Nielsen, P. C. Ragas, J. S. Mattick, *Science* **2002**, *295*, 1487.
[10] J. N. Wiking, V. Zaburdaev, M. D. Volder, R. Losick, M. P. Brenner, D. A. Weitz, *Proc. Natl. Acad. Sci. USA* **2013**, *110*, 848.
[11] A. Houry, M. Gohar, J. Deschamps, E. Tischenko, S. Aymerich, A. Gruss, R. Briandet, *Proc. Natl. Acad. Sci. USA* **2012**, *109*, 13088.
[12] K. Ulbrich, K. Holá, V. Šubr, A. Bakandritsos, J. Tuček, R. Zbořil, *Chem. Rev.* **2016**, *116*, 5338.
[13] L. Li, P. Yu, X. Wang, S. Yu, J. Mathieu, H. Yu, P. J. J. Alvarez, *Environ. Sci.: Nano* **2017**, *4*, 1817.
[14] G. Hwang, A. J. Paula, E. E. Hunter, Y. Liu, A. Babeer, B. Karabucak, K. Stebe, V. Kumar, E. Steager, H. Koo, *Sci. Rob.* **2019**, *4*, eaaw2388.
[15] C. Zhang, C. Du, J. Liao, Y. Gu, Y. Gong, J. Pei, H. Gu, D. Yin, L. Gao, Y. Pan, *Biomater. Sci.* **2019**, *7*, 2833.
[16] M. J. Hajipour, K. M. Fromm, A. A. Ashkarran, D. J. Aberasturi, I. R. Larramendi, T. Rojo, V. Serpooshan, W. J. Parak, M. Mahmoudi, *Trends Biotechnol.* **2012**, *30*, 499.
[17] W. Cheng, K. Tang, Y. Qi, J. Sheng, Z. Liu, *J. Mater. Chem.* **2010**, *20*, 1799.
[18] T. G. Emori, R. P. Gaynes, *Clin. Microbiol. Rev.* **1993**, *6*, 428.
[19] T. Møretrø, L. Hermansen, A. L. Holck, M. S. Sidhu, K. Rudi, S. Langsrud, *Appl. Environ. Microbiol.* **2003**, *69*, 5648.
[20] H. N. Rasyid, H. C. van der Mei, H. W. Frijlink, S. Soegijoko, J. R. van Horn, H. J. Busscher, D. Neut, *Acta Orthop.* **2009**, *80*, 508.
[21] T. Bjarnsholt, M. Alhede, M. Alhede, S. R. Eickhardt-Sørensen, C. Moser, M. Kühl, P. Ø. Jensen, N. Høiby, *Trends Microbiol.* **2013**, *21*, 466.
[22] J. G. E. Hendriks, D. Neut, J. R. van Horn, H. C. van der Mei, H. J. Busscher, *J. Biomed. Mater. Res., Part B* **2003**, *64*, 1.
[23] H. J. Busscher, V. Alt, H. C. van der Mei, P. H. Fagette, W. Zimmerli, T. F. Moriarty, J. Parvizi, G. Schmidmaier, M. J. Raschke, T. Gehrke, R. Bayston, L. M. Baddour, L. C. Winterton, R. O. Darouiche, D. W. Grainger, *ACS Biomater. Sci. Eng.* **2019**, *5*, 402.
[24] L. Gogokhia, K. Buhrke, R. Bell, B. Hoffman, D. G. Brown, C. H. Gogokhia, N. J. Ajami, M. C. Wong, A. Ghazaryan, J. F. Valentine, N. Porter, E. Martens, R. O'Connell, V. Jacob, E. Scherl, C. Crawford, W. Z. Stephens, S. R. Casjens, R. S. Longman, J. L. Round, *Cell Host Microbe* **2019**, *25*, 285.
[25] C. Loc-Carrillo, S. T. Abedon, *Bacteriophage* **2011**, *1*, 111.
[26] T. Tang, X. Sun, X. Xu, Y. Bian, X. Ma, N. Chen, *RSC Adv.* **2019**, *9*, 2559.
[27] G. Jarockyte, E. Daugelaite, M. Stasys, U. Statkute, V. Poderys, T. Tseng, S. Hsu, V. Karabanovas, R. Rotomskis, *Int. J. Mol. Sci.* **2016**, *17*, 1193.